Single-ion BAB triblock copolymers as highly efficient electrolytes for lithium-metal batteries

Renaud Bouchet, Sébastien Maria, Rachid Meziane, Abdelmaula Aboulaich, Livie Liénafa, Jean-Pierre Bonnet, Trang N T Phan, Denis Bertin, Didier Gigmes, Didier Devaux, et al.

Single-ion BAB triblock copolymers as highly efficient electrolytes for lithium-metal batteries

Renaud Bouchet[1]*[†], Sébastien Maria[2], Rachid Meziane[3], Abdelmaula Aboulaich[1†], Livie Lienafa[2], Jean-Pierre Bonnet[3], Trang N. T. Phan[2], Denis Bertin[2], Didier Gigmes[2], Didier Devaux[1], Renaud Denoyel[1] and Michel Armand[3]

Electrochemical energy storage is one of the main societal challenges of this century. The performances of classical lithium-ion technology based on liquid electrolytes have made great advances in the past two decades, but the intrinsic instability of liquid electrolytes results in safety issues. Solid polymer electrolytes would be a perfect solution to those safety issues, miniaturization and enhancement of energy density. However, as in liquids, the fraction of charge carried by lithium ions is small (<20%), limiting the power performances. Solid polymer electrolytes operate at 80 °C, resulting in poor mechanical properties and a limited electrochemical stability window. Here we describe a multifunctional single-ion polymer electrolyte based on polyanionic block copolymers comprising polystyrene segments. It overcomes most of the above limitations, with a lithium-ion transport number close to unity, excellent mechanical properties and an electrochemical stability window spanning 5 V versus Li^+/Li. A prototype battery using this polyelectrolyte outperforms a conventional battery based on a polymer electrolyte.

Climate change, pollution and declining fossil resources are overwhelming challenges to mankind. The development of alternative transportation such as fully electric or hybrid vehicles has become a key need for sustainable long-term development[1]. The challenge in the very near future is to find a safe, cheap and efficient battery technology that would enable electric vehicles an extended driving range (>350 km). The corresponding increase in energy density requires the development of new chemistries for both the active electrode materials and the electrolyte[2,3]. Lithium metal as the anode is the ultimate negative electrode and the only choice to complement the positive air (O_2) or sulphur cathodes to really take advantage of the high specific capacities of these cathodes[4]. However, the use of lithium metal in contact with a liquid electrolyte unfortunately leads to safety problems associated with the formation of irregular metallic lithium electrodeposits during the recharge, which results in dendrite formation responsible for explosion hazards. Solid-state electrolytes would be a perfect solution[5] to mitigate the lithium dendritic growth. Inorganic lithium ion conductors generally based on LISI-CON type material are still in development because they are not stable in contact with lithium[4]. The use of a solid polymer electrolyte (SPE), which is a lithium salt associated with a polar polymer matrix without organic solvents, could solve most of the safety issues encountered with liquid electrolytes. However, the development of SPEs has been hampered by two issues: the inability to design a SPE that has both a high ionic conductivity and good mechanical properties[6] and the fact that the motion of lithium ions carries only a small fraction (1/5th) of the overall ionic current, which leads during battery operation to the formation of a strong concentration gradient with deleterious effects such as favoured dendritic growth[7] and limited power delivery. Here we describe a new single-ion polymer electrolyte based on self-assembled polyanionic BAB triblock copolymers (see Fig. 1) to finely tune mechanical properties, ionic conductivity and lithium transport number at the same time. The B block is a polyelectrolyte based on poly(styrene trifluoromethane-sulphonylimide of lithium) P(STFSILi) associated with a central A block based on a linear poly(ethylene oxide) (PEO). The single-ion conductivity (1.3×10^{-5} S cm^{-1} at 60 °C) is almost half an order of magnitude higher than that of the state-of-the-art[8] value for such materials and is combined with a markedly improved mechanical strength. The electrochemical stability window is extended up to 5 V versus Li^+/Li and battery tests show that the power performances and cycling are outstanding particularly at 60 °C, which makes these materials highly attractive for the next generation of batteries.

Li-ion batteries are much too expensive to meet the requirements of the electric vehicle mass market and their safety is limited[9] owing to the use of liquid or liquid-based electrolytes showing thermal instability[10], with flammable reaction products, the possibility of leaks, and internal short-circuits. SPEs present several advantages: the lamination (Li metal, electrolyte, composite cathode), stacking and hermetic sealing processes are much simpler and cost-effective with a polymer electrolyte. Polymers are indeed robust, lightweight, flame-resistant and can be shaped to suit the requirements of the application.

Many polymer/lithium salt systems have been considered and the most widely studied and used system is the bis(trifluoromethanesulphonyl)imide lithium salt ($LiN(SO_2CF_3)_2$ or LiTFSI), dissolved in an aprotic polymer matrix of PEO. PEO contains ether coordination sites that enable the dissociation of salts, together with a flexible macromolecular structure that assists ionic transport. Nevertheless, the presence of PEO crystalline regions interferes with ion transport, which requires an amorphous phase[11]. This affects the ionic conductivity at temperatures below the melting temperature of around 65 °C. Above the melting
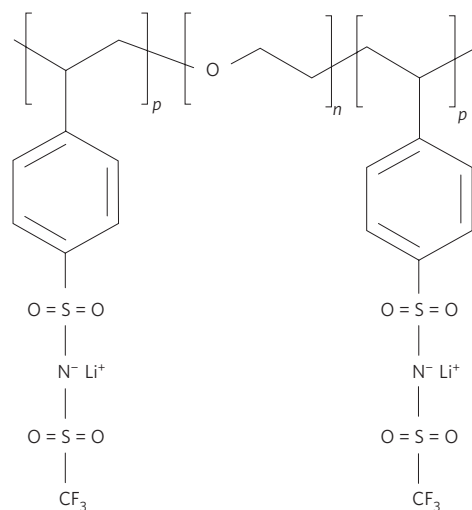
Figure 1 | Chemical structure of the single-ion conductor triblock copolymer P(STFSILi)-b-PEO-b-P(STFSILi) proposed as an electrolyte for lithium-metal-based batteries.
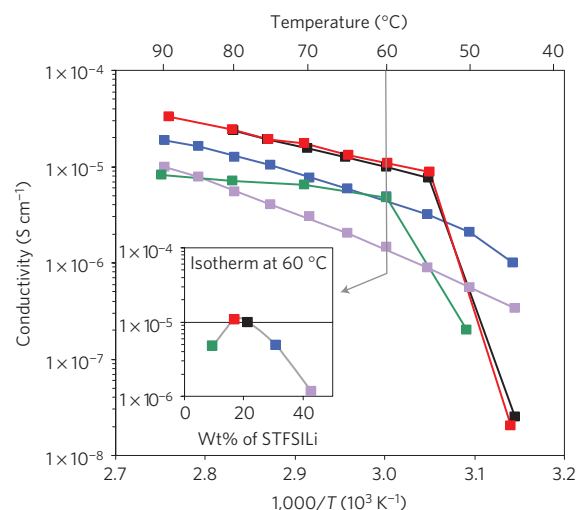

Figure 2 | Conductivity performances. Plots of conductivity as a function of inverse temperature for several P(STFSILi)-PEO-P(STFSILi) A-BCEs. Inset: isothermal conductivity at 60 °C according to the wt% of the P(STFSILi) block.

temperature of PEO, the ionic conductivity strongly increases, but at these temperatures, PEO becomes a viscous liquid and loses its dimensional stability. Various approaches have been used to suppress crystallization and strengthen the mechanical properties of PEO by the addition of hard colloidal particles[12–17], by increasing the molar mass of PEO or by crosslinking, but these have often caused a decrease in ionic conductivity. Similarly, attempts to improve the conductivity of PEO by adding plasticizers have led to the deterioration of mechanical properties[18]. Finally it was shown that at the operating temperature of these SPEs (that is, 80–100 °C), PEO electrolytes do not hamper dendritic growth[19,20].

To combine in the same material these two antagonistic properties (mechanical and conductivity), block copolymer electrolytes (BCE) have recently been proposed as SPEs (refs 21–27). The most common architectures are the AB diblock and BAB triblock copolymers, where A is the ionic conductor block and B is the block providing the mechanical strength. The A block generally consists of either a linear PEO block[21,22] or a low-molecular-weight poly(ethylene glycol) block grafted on a macromolecular backbone such as poly(ethylene glycol methacrylate)[23–27]. For the mechanical reinforcement block, a wide variety of polymers have been tested including polystyrene[21] and poly(alkyl methacrylates)[23]. Even though a better compromise between mechanical and conductivity properties has been obtained using such a strategy, these BCEs present a significant power limitation due to the small current fraction carried by the lithium cations (measured by the transport number t^+) into the PEO conducting phase ($t^+ \sim 0.1$–0.2; ref. 28). During the discharge of the battery, lithium ions are indeed over-concentrated at the negative electrode and depleted at the positive electrode, leading to the formation of a concentration gradient that limits the maximum current available owing to the diffusion of ions generating important osmotic forces. Conversely, during the charge, the development of metallic dendrites is expected when the lithium ion concentration decreases to zero at the lithium electrolyte interface[7]. Mostly to overcome these power limitations, only recently the use polyanionic block copolymers to create a single-ion conductor SPE was proposed[26]. A large study of a variety of graft-diblock copolymers has subsequently been carried out[8,24,29–31] using carboxylates and sulphonates as anions. A t^+ value of 0.9 on a poly(lauryl methacrylate-co-lithium methacrylate)-b-poly(ω-methoxy-polyethylene glycol) electrolyte was obtained. However, this material has a very low conductivity (below 5×10^{-6} S cm^{-1} at 60 °C) mostly owing to the low level of ionic dissociation.

Here we have designed a single-ion conductor based on a polyanionic BCE (denoted in the following parts as A-BCE) using the well-known TFSI anion, whose structure enables an important delocalization of the negative charge. Therefore, Li$^+$ has weak interactions with this anionic structure, consequently enabling a high dissociation level. Table 1 lists the synthesized A-BCEs together with their molecular weights, compositions and equivalent molar ratios [EO]/[Li].

The ionic conductivities of anionic block copolymer electrolytes (A-BCE) with different proportions of P(STFSILi) (9.5, 17, 21.4, 31 and 43 wt% respectively) are shown in Fig. 2a in an Arrhenius plot. A drop in conductivity of several orders of magnitude is observed for the A-BCEs with 9.5, 17 and 21.4 wt% P(STFSILi) (at a temperature below 60 °C for the 9.5 wt%, and 55 °C for the 17 and 21.4 wt% P(STFSILi) A-BCEs) due to PEO crystallization. Interestingly, this knee disappears when the amount of (PSTFSILi) increases (31 wt% and beyond), suggesting both a decrease in the melting temperature and in the degree of crystallinity. These results are confirmed by differential scanning calorimetry (Supplementary Fig. S2 and Table S2). The maximum ionic conductivity (Fig. 2b) is observed at about 20 wt% P(STFSILi), which corresponds to an ethylene oxide/lithium molar ratio ([EO]/[Li]) of approximately 30. This value is higher than the one obtained with the PEO directly laden with LiTFSI salt[32] ([EO]/[Li] = 20) because dissociable Li–TFSI functions are located at the interface between the P(STFSILi) and PEO domains (that is, a two-dimensional conformation as opposed to bulk three-dimensional complexation), but on the other hand the forced separation between the B block containing the counter anion from the lithium-solvating PEO block has been shown to improve ion dissociation[24]. The former will depend on the surface to volume ratio of the polymer domain, which is linked to the morphology adopted during the phase nano-separation, thus depending on the ratio of A to B blocks[33]. Whatever the case, the conductivity reaches a value of 1.3×10^{-5} S cm^{-1} at 60 °C (Fig. 2b), which is a superior result for a single-ion polymer conductor. The transport number of these materials was measured by impedance spectroscopy using the relationship proposed in ref. 34 (Supplementary Fig. S3) and reaches values greater than 0.85, slightly below the expected value of unity. In the copolymer, the anion is grafted on the polymer backbone such that it cannot move in a long range. Therefore, structurally our materials contain only one mobile charge, which is the lithium

Table 1 | Molecular weights and compositions of synthesized PSTFSILi-PEO-PSTFSILi triblock copolymers.

Sample	M_n (PEO) g mol^{-1}	M_n (PSTFSILi) g mol^{-1}	M_n (total) g mol^{-1}	Wt% of PSTFSILi	[EO]/[Li]*
A-BCE_1		2×1850	38,700	9.5	69
A-BCE_2		2×3600	42,200	17	36
A-BCE_3	35,000	2×4750	44,500	21.4	27
A-BCE_4		2×7800	50,600	31	16
A-BCE_5		2×13200	61,400	3	10

*Molar ratio was calculated from the block copolymer compositions determined by ^{1}H NMR compositional analysis of the final copolymer.
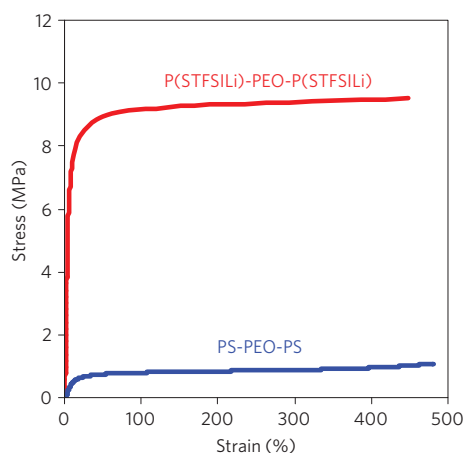

Figure 3 | Mechanical performances. Comparative tensile tests at 40 °C for the neutral copolymer PS-PEO-PS with 25 wt% PS loaded with LiTFSI at [EO]/[Li] = 30 (blue curve) and the copolymer P(STFSILi)-PEO-P(STFSILi) with 31 wt% P(STFSILi) (red curve).

cation (when dissociated from the anion); by design the cationic transport number is unity. This value should be considered as a minimum value; the low-frequency diffusion process observed by impedance spectroscopy can be due to the passive layers present on the lithium surface.

Stress–strain tests at 40 °C on an A-BCE P(STFSILi)-PEO-P(STFSILi) copolymer with 31 wt% P(STFSILi) compared with a neutral triblock copolymer polystyrene-PEO-polystyrene (PS-PEO-PS, 25 wt% of PS) laden with LiTFSI at [EO]/[Li] = 30 are shown in Fig. 3 (the results obtained at 60 °C are given in Supplementary Fig. S4). These copolymers have the same central PEO block, that is, 35 kg mol^{-1}, with almost the same composition in wt%. The difference here comes from the nature of the B block. Compared with the neutral BCE, which undergoes a phase nano-separation that improves its mechanical properties compared with the PEO homopolymer, the A-BCE presents a tensile stress an order of magnitude higher when we move from PS-PEO-PS to P(STFSILi)-PEO-P(STFSILi). This remarkable effect is therefore not only the result of the phase nano-separation, but also an indication of a strong ionic crosslinking between the anionic and PEO domains believed to induce self-healing in some ionomer-type polymers[35]. This unique property will be of great benefit for the long-time operation of batteries as one of the ageing mechanisms is due to the loss of interfacial contact induced by the repeated volume variations of active materials during lithium intercalation/de-intercalation (that is, charge/discharge). Moreover, these excellent mechanical properties are also expected to mitigate the dendritic growth of lithium metal.

The electrochemical stability of these single-ion block copolymers was analysed by cyclic voltammetry using Li/A-BCE/stainless-steel cells. The measurements were performed at 80 °C between
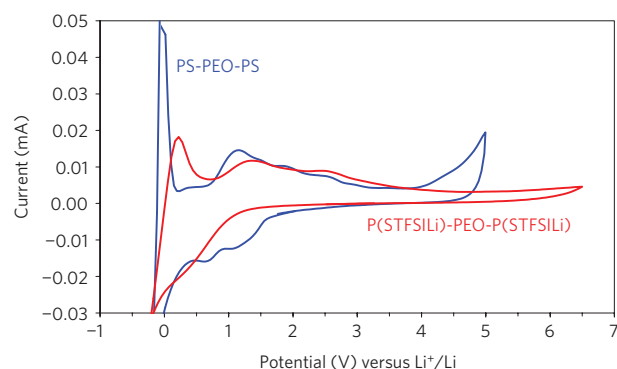

Figure 4 | Electrochemical stability window. Voltammogram obtained at 1 mV s^{-1} for the A-BCE with 31 wt% P(STFSILi) (red curve) at 80 °C. For comparison, the voltammogram obtained in the same conditions with the neutral copolymer PS-PEO-PS with 30 wt% PS laden with LiTFSI at [EO]/[Li] = 25 (blue curve) is also given.

−0.2 and 6.5 V (versus Li$^+$/Li) at a scan rate of 1 mV s^{-1}. The results are shown in Fig. 4. The A-BCEs are stable up to at least 5 V versus Li$^+$/Li, which is appreciably wider than their counterparts based on salt-laden PEO homopolymers (stability up to 3.8 V versus Li$^+$/Li (ref. 36) as shown for comparison in Fig. 4). This result is consistent with the fact that instability at high potential is due to anions[37], which in our case are tethered to the polymer chain and can lose their negative charge only at the interface. The consequence here is an enhanced electrochemical stability. Therefore, this A-BCE electrolyte makes it possible to consider the use of high-potential cathode materials[3] that cannot be safely tested in liquid electrolytes owing to their lower electrochemical stability.

Finally, to further confirm the usefulness of these new electrolytes, battery prototypes based on A-BCEs (31 wt% P(STFSILi)) were assembled using a lithium-metal negative electrode (anode) and a carbon-coated LiFePO$_4$ as a model active material for the positive electrode (cathode). The formulation of the composite cathodes was 60 wt% LiFePO$_4$, 32 wt% A-BCE and 8 wt% carbon black. The composite electrode was about 70 μm thick with an estimated porosity of 45% (see Fig. 5a), which is a strong disadvantage in an all solid-state technology as it makes the average ion pathway longer and more tortuous. However, the aim of this work is to demonstrate a proof of concept, not the technical optimization of the electrode formulation and processing, which was beyond our means. Cycling tests were conducted at different temperatures (60, 70 and 80 °C) and different power rates where the rate is denoted C/n corresponding here to a full discharge (respectively, full charge) of the theoretical cathode capacity (C) in n hours. Figure 5b shows a characteristic evolution at 80 °C of the battery voltage for different rates obtained for a typical Li/A-BCE/LiFePO$_4$ prototype as a function of the capacity stored by the positive active material (theoretically 170 mAh g^{-1} for LiFePO$_4$). Up to a C/2 rate a well-defined potential plateau is observed, with a polarization
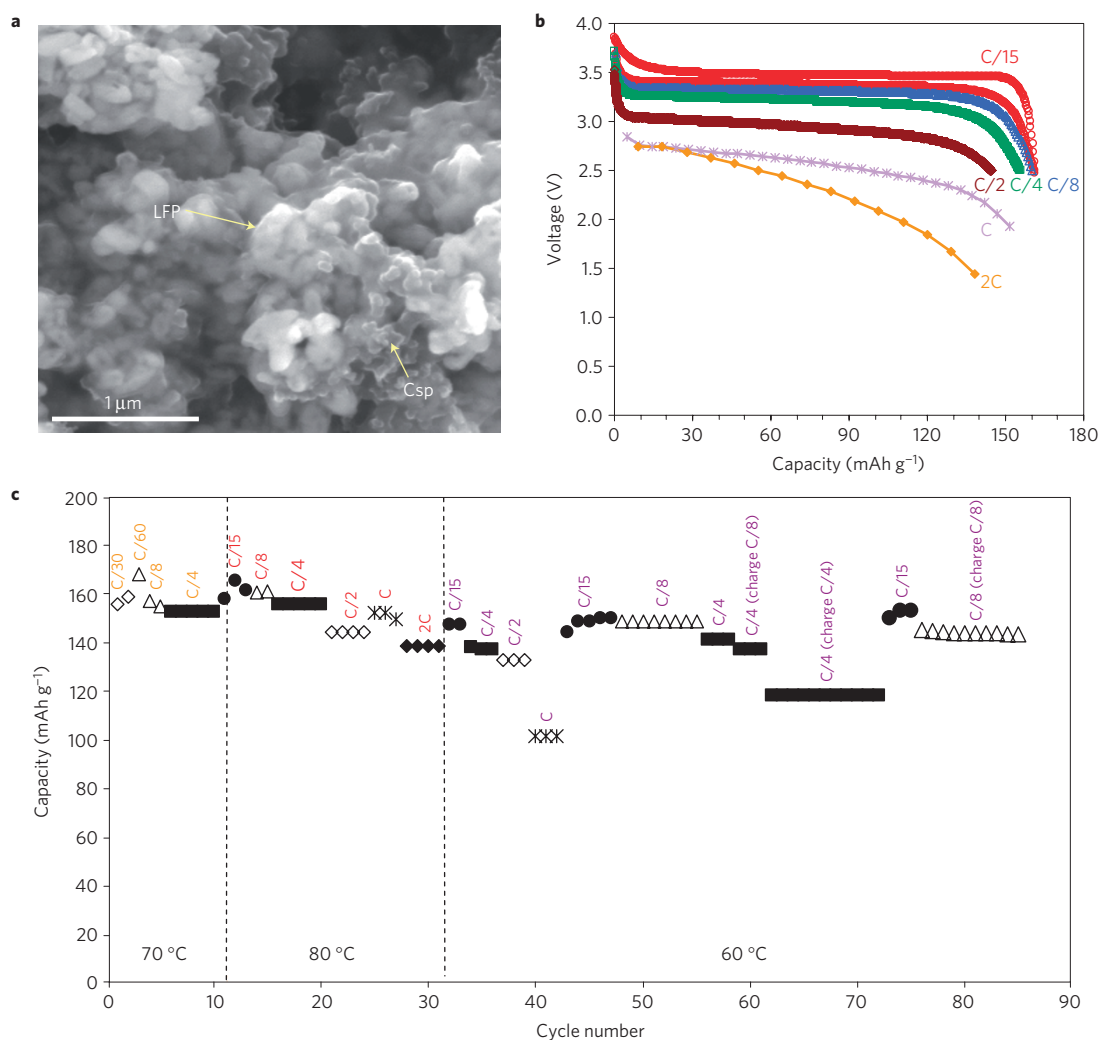
Figure 5 | Cyclability. a, A scanning electron micrograph of the bulk of the composite electrode. **b**, Discharge profiles obtained at 80 °C at different rates from C/15 to 2C for a typical prototype Li/A-BCE/LiFePO$_4$. **c**, Cycle-life of the prototype. The different temperatures and C/n rates used are noted in the figure.

proportional to the rate. Above this rate, transport limitations mostly due to the porosity of the composite electrode start to be observed although the capacity retention is still 138 mAh g^{-1} at 2C. The cycle-life data of the prototype, which correspond to the returned capacity as a function of the cycle number for the different rates at three different temperatures, are shown in Fig. 5c. More than 80 cycles are observed without any capacity-fading regardless of the temperature (60, 70 and 80 °C) and rate, revealing attractive performances compared with the literature results with lithium-metal batteries using dry polymer electrolytes[38]. The cyclability at 60 °C with more than 50 stable cycles is particularly noticeable. This is especially impressive because, in the presented data, it is the same prototype cell that cycled in different thermal conditions, which is a harsh treatment because the tests are usually isothermal, except for a simulation of accelerated ageing.

The power holding capacity of these prototypes given by the discharged capacity as a function of the C/n rate is shown in Fig. 6. There is retention of more than 85% of the capacity at a C/2 rate, whatever the temperature between 60 and 80 °C. To our knowledge there is no dry polymer battery technology with such outstanding behaviour. In particular, the results at 60 °C are interesting as they hint at the possibility of a working temperature with comparable performances 20 °C below the standard one (80 °C) used for state-of-the-art dry SPEs (refs 39,40). Typically, these results are related to
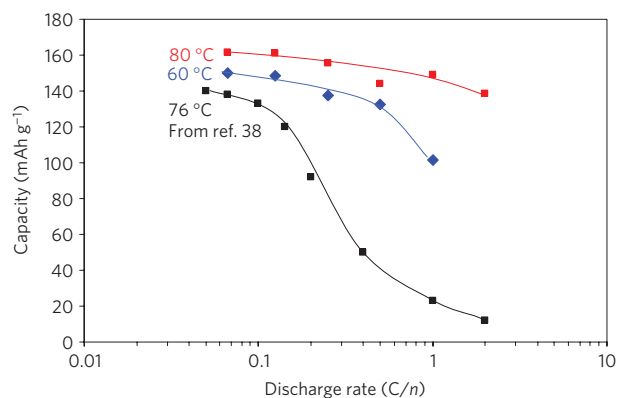
Figure 6 | Discharged capacity according to the discharge rate compared at 60 and 80 °C. The data are taken from Fig. 5c. The black data taken from ref. 38 are for comparison with state-of-the-art performances.

two facts. The electrolyte placed between the negative and positive electrodes, and also in the composite cathode, has a cation transport number approaching unity while having a reasonable conductivity (that is, not too penalizing in terms of polarization). This prevents during cycling the formation of concentration gradients (in the

electrolyte and electrode) that usually limit strongly battery power and favour lithium dendritic growth. Finally, the use of the new A-BCE promises safety because the material is stable up to 350 °C (Supplementary Fig. S5) and even in the charged state cathode where catalytic degradation reactions can occur, the stability of the A-BCE is unchanged.

In this Article, we report a P(STFSILi)-PEO-P(STFSILi) material as a polymer electrolyte exhibiting unprecedented levels of performance for lithium-metal batteries in terms of ionic conductivity of dry single-ion polymer electrolytes (1.3×10^{-5} S cm^{-1} at 60 °C), transport number (>0.85) and improved mechanical strength compared with the neutral PS-POE-PS triblock copolymer (10 MPa at 40 °C), and enlarged electrochemical stability window compared with PEO (up to 5 V versus Li$^+$/Li). Owing to the combination of all these relevant properties, using this material as a SPE and in the formulation of the composite cathode, we have been able to elaborate lithium-metal battery prototypes with an impressive gain in power performances compared with state-of-the-art lithium-metal battery technology, particularly at 60 °C. We believe this paves the way for the design and elaboration of a new class of macromolecular electrolytes that will address the bottlenecks in the development of future lithium-metal-based battery technology for electric transport.

Methods

Materials. Oxalyl chloride, 4-styrenesulphonic acid sodium salt, triethylamine, 4-dimethylaminopyridine and PEO with a molar mass of 35,000 gmol^{-1} were all obtained from Aldrich and used as received. The trifluoromethanesulphonamide was obtained from Rhodia. All solvents and other reagents were synthesis grade and used without further purification.

Single-ion block copolymer synthesis. The lithium 4-styrenesulphonyl(trifluoromethylsulphonyl) imide (STFSILi) was synthesized according to the modified method of ref. 41 starting from trifluoromethanesulphonamide and 4-styrene sulphonyl chloride. Batches of polyanionic P(STFSILi)-PEO-P(STFSILi) block copolymers with different ratios of P(STFSILi)/PEO (10 to 40 wt% P(STFSILi)) were synthesized by the nitroxide-mediated polymerization (NMP) method. The wt% of the P(STFSILi) block in the copolymer was determined by ^{1}H NMR (see Table 1). Experimental details of the synthesis and characterization of block copolymers are described in the Supplementary Information. The synthesis of the neutral PS-PEO-PS triblock copolymer consisted of three steps following previously reported procedures[42,43]. Briefly, the first step is the esterification of the PEO α, ω-dihydroxyls with acryloyl chloride to form the corresponding PEO diacrylate. The second step corresponds to the 1,2 intermolecular radical addition of the BlocBuilder[44] onto the acrylate group to yield the corresponding PEO-based macroalkoxyamines. The third step is the solution nitroxide-mediated polymerization of styrene using PEO-based macroalkoxyamines as the initiator at 110 °C.

Electrolyte film preparation. For the ionic conductivity and mechanical traction measurements, thin films of single-ion BCE were produced using the casting method. First, 10 wt% of the polymers was dissolved in pure water. The solution was then cast on a polypropylene film. After room-temperature water removal, the resulting films were further dried in a vacuum oven at 50 °C for 24 h and stored in a dry-argon filled glove box (<3 ppm H$_2$O) for at least 1 week before any experiment. The film thicknesses were in the range 70–100 μm.

Ionic conductivity and transport number. Symmetrical lithium/BCE/lithium cells were assembled in the glove box through a lamination process and then sealed in a hermetic coffee bag to carry out impedance spectroscopy measurements as a function of temperature in the range 20–90 °C in a Vötsch oven. The conductivity and transport number were measured by impedance spectroscopy using a Solartron frequency analyser 1260. The frequency range was 10^7) to 10^{-3} Hz and the signal amplitude was 20 mV.

Mechanical properties. Traction tests were performed using a DMA Q800 (TA Instruments) to evaluate Young's modulus and the tensile stress. The samples were stamped out from the films prepared for conductivity in the shape of a rectangle 6 mm wide and 20 mm long. The machine is equipped with a mobile oven that controls the temperature of the sample. The sample was positioned in between the two clamps of the machine and then the oven was positioned. A flow of 20 l min^{-1} of dry air was used to prevent water uptake of the samples. Before the traction the sample was heated to 40 °C and dried for 1 h. Finally a ramp force of 0.1 N min^{-1} was applied until the sample broke.

Electrochemical characterization. To analyse the electrochemical stability window lithium/A-BCE/stainless-steel cells were assembled in the glove box through a lamination process. The electrochemical cells were sealed in a coffee bag to carry out the experiments outside the glove box. The cells were equilibrated at 80 °C in a Memmert oven. Then cyclic voltammetries at 1 mV s^{-1} between −0.2 V and 6.5 V versus Li$^+$/Li were carried out using a Solartron multipostensiostat 1470 driven by Corware software (Scribner).

Battery tests. Carbon-coated LiFePO$_4$ active materials were used to formulate the composite cathode. Carbon black (C$_{65}$ from Timcal) was used to ensure the electronic percolation into the electrode volume. A composition of 60/32/8 (weight%) of LFP/A-BCE/C$_{65}$ was used. A mixture of the components with water enabled the production of an ink that was casted onto a surface-treated aluminium current collector. The surface capacity was about 0.8 mAh cm^{-2}. After evaporation of water at room temperature a composite electrode was obtained. Further drying in a vacuum oven at 50° C for 24 h was done before the cathode was stored for one week in the glove box. Finally, lithium/A-BCE/cathode batteries were assembled through lamination processes and sealed in a coffee bag. Batteries were cycled using a Solartron 1470 multipotentiostat. The potential window was 3.8 V to 2.5 V for regimes below C/2; the lower potential limit is decreased to 2 V at D and 1.5 V at 2C. The charge is always C/15 unless specified otherwise in the main text.

References

1. Tollefson, J. Car industry: Charging up the future. *Nature* **456,** 436–440 (2008).
2. Cheng, F., Liang, J., Tao, Z. & Chen, J. Functional materials for rechargeable batteries. *Adv. Mater.* **23,** 1695–1715 (2011).
3. Armand, M. & Tarascon, J-M. Building better batteries. *Nature* **451,** 652–657 (2008).
4. Bruce, P. G., Freunberger, S. A., Hardwick, L. J. & Tarascon, J-M. Li–O$_2$ and Li–S batteries with high energy storage. *Nature Mater.* **11,** 19–29 (2012).
5. Murata, K., Izuchi, S. & Yoshihisa, Y. An overview of the research and development of solid polymer electrolyte batteries. *Electrochim. Acta* **45,** 1501–1508 (2000).
6. Bruce, P. G. & Vincent, C. A. Polymer electrolytes. *J. Chem. Soc. Faraday Trans.* **89,** 3187–3203 (1993).
7. Chazalviel, J-N. Electrochemical aspects of the generation of ramified metallic electrodeposits. *Phys. Rev. A* **42,** 7355–7367 (1990).
8. Ryu, S. W. *et al.* Effect of counter ion placement on conductivity in single-ion conducting block copolymer electrolytes. *J. Electrochem. Soc.* **152,** A158–A163 (2005).
9. Goodenough, J. B. & Kim, Y. Challenges for rechargeable Li batteries. *Chem. Mater.* **22,** 587–603 (2010).
10. Hammami, A., Raymond, N. & Armand, M. Lithium-ion batteries: Runaway risk of forming toxic compounds. *Nature* **424,** 635–636 (2003).
11. Marzantowicz, M., Dygas, J. R., Krok, F., Florjańczyk, Z. & Zygadło-Monikowska, E. Influence of crystalline complexes on electrical properties of PEO:LiTFSI electrolyte. *Electrochim. Acta* **53,** 1518–1526 (2007).
12. Vaia, R. A., Vasudevan, S., Krawiec, W., Scanlon, L. G. & Giannelis, E. P. New polymer electrolyte nanocomposites: Melt intercalation of poly(ethylene oxide) in mica-type silicates. *Adv. Mater.* **7,** 154–156 (1995).
13. Wong, S. & Zax, D. B. What do NMR linewidths tell us? Dynamics of alkali cations in a PEO-based nanocomposite polymer electrolyte. *Electrochim. Acta* **42,** 3513–3518 (1997).
14. Bujdàk, J., Hackett, E. & Giannelis, E. P. Effect of layer charge on the intercalation of poly(ethylene oxide) in layered silicates: Implications on nanocomposite polymer electrolytes. *Chem. Mater.* **12,** 2168–2174 (2000).
15. Capiglia, C., Mustarelli, P., Quartarone, E., Tomasi, C. & Magistris, A. Effects of nanoscale SiO$_2$ on the thermal and transport properties of solvent-free, poly(ethylene oxide) (PEO)-based polymer electrolytes. *Solid State Ion.* **118,** 73–79 (1999).
16. Croce, F., Appetecchi, G. B., Persi, L. & Scrosati, B. Nanocomposite polymer electrolytes for lithium batteries. *Nature* **394,** 456–458 (1998).
17. Forsyth, M. *et al.* The effect of nano-particle TiO$_2$ fillers on structure and transport in polymer electrolytes. *Solid State Ion.* **147,** 203–211 (2002).
18. Manuel Stephan, A. Review on gel polymer electrolytes for lithium batteries. *Eur. Polymer J.* **42,** 21–42 (2006).
19. Dollé, M., Sannier, L., Beaudoin, B., Trentin, M. & Tarascon, J-M. Live scanning electron microscope observations of dendritic growth in lithium/polymer cells. *Electrochem. Solid-State Lett.* **5,** A286–A289 (2002).
20. Rosso, M. *et al.* Dendrite short-circuit and fuse effect on Li/polymer/Li cells. *Electrochim. Acta* **51,** 5334–5340 (2006).
21. Singh, M. *et al.* Effect of molecular weight on the mechanical and electrical properties of block copolymer electrolytes. *Macromolecules* **40,** 4578–4585 (2007).

22. Panday, A. *et al*. Effect of molecular weight and salt concentration on conductivity of block copolymer electrolytes. *Macromolecules* **42,** 4632–463 (2009).

23. Soo, P. P. *et al*. Rubbery block copolymer electrolytes for solid-state rechargeable lithium batteries. *J. Electrochem. Soc.* **146,** 32–37 (1999).

24. Trapa, P. E., Huang, B., Won, Y-Y., Sadoway, D. R. & Mayes, A. M. Block copolymer electrolytes synthesized by atom transfer radical polymerization for solid-state, thin-film lithium batteries. *Electrochem. Solid-State Lett.* **5,** A85–A88 (2002).

25. Trapa, P. E. *et al*. Rubbery graft copolymer electrolytes for solid-state, thin-film lithium batteries. *J. Electrochem. Soc.* **152,** A1–A5 (2005).

26. Sadoway, D. R. Block and graft copolymer electrolytes for high-performance, solid-state lithium batteries. *J. Power Sources* **129,** 1–3 (2004).

27. Niitani, T. *et al*. Synthesis of Li$^+$ ion conductive PEO-PSt block copolymer electrolyte with microphase separation structure. *Electrochem. Solid-State Lett.* **8,** A385–A388 (2005).

28. Hayamizu, K., Akiba, E., Bando, T. & Aihara, Y. ^{1}H, ^{7}Li, and ^{19}F nuclear magnetic resonance and ionic conductivity studies for liquid electrolytes composed of glymes and polyetheneglycol dimethyl ethers of $CH_3O(CH_2CH_2O)_nCH_3$ ($n = 3$–50) doped with $LiN(SO_2CF_3)_2$. *J. Chem. Phys.* **117,** 5929–5939 (2002).

29. Mayes, A., Sadoway, D. R. & Bannerjee, P. Block copolymer electrolyte. Patent WO 00/05774 (2000).

30. Sadoway, D. R. *et al*. Self-doped block copolymer electrolytes for solid-state, rechargeable lithium batteries. *J. Power Sources* **97–98,** 621–623 (2001).

31. Hu, Q. *et al*. Graft copolymer-based lithium-ion battery for high-temperature operation. *J. Power Sources* **196,** 5604–5610 (2011).

32. Meyer, W. H. Polymer electrolytes for lithium-ion batteries. *Adv. Mater.* **10,** 439–448 (1998).

33. Abetz, V. & Simon, P. F. W. Phase behaviour and morphologies of block copolymers. *Adv. Polym. Sci.* **189,** 125–212 (2005).

34. MacDonald, J. R. Binary electrolyte small-signal frequency response. *Electroanal. Chem. Int. Electrochem.* **53,** 1–55 (1974).

35. Wu, D. Y., Meure, S. & Solomon, D. Self-healing polymeric materials: A review of recent developments. *Prog. Polym. Sci.* **33,** 479–522 (2008).

36. Siqueira, L. J. A. & Ribeiro, M. C. C. Molecular dynamics simulation of the polymer electrolyte poly(ethyleneoxide)/LiClO$_4$. I. Structural properties. *J. Chem. Phys.* **122,** 194911 (2005).

37. Armand, M. Polymer solid electrolytes—an overview. *Solid State Ion.* **9–10,** 745–754 (1983).

38. Croce, F., Sacchetti, S. & Scrosati, B. Advanced, lithium batteries based on high-performance composite polymer electrolytes. *J. Power Sources* **162,** 685–689 (2006).

39. Wang, L., Li, X. & Yang, W. Enhancement of electrochemical properties of hot-pressed poly(ethylene oxide)-based nanocomposite polymer electrolyte films for all-solid-state lithium polymer batteries. *Electrochim. Acta* **55,** 1895–1899 (2010).

40. Kaneko, F. *et al*. Capacity fading mechanism in all solid-state lithium polymer secondary batteries using PEG-borate/aluminate ester as plasticizer for polymer electrolytes. *Adv. Funct. Mater.* **19,** 918–925 (2009).

41. Meziane, R., Bonnet, J-P., Courty, M., Djellab, K. & Armand, M. Single-ion polymer electrolytes based on a delocalized polyanion for lithium batteries. *Electrochim. Acta* **57,** 14–19 (2011).

42. Bloch, E., Phan, T., Bertin, D., Llewellyn, P. & Hornebecq, V. Direct synthesis of mesoporous silica presenting large and tunable pores using BAB triblock copolymers: Influence of each copolymer block on the porous structure. *Micropor. Mesopor. Mater.* **112,** 612–620 (2008).

43. Girod, M., Phan, T. N. T. & Charles, L. Microstructural study of a nitroxide-mediated poly(ethylene oxide)/polystyrene block copolymer (PEO-b-PS) by electrospray tandem mass spectrometry. *J. Am. Soc. Mass Spectrom.* **19,** 1163–1175 (2008).

44. Gigmes, D. *et al*. Intermolecular radical 1,2-addition of the BlocBuilder MA alkoxyamine onto activated olefins: A versatile tool for the synthesis of complex macromolecular architecture. *Polym. Chem.* **2,** 1624–1631 (2011).

Author contributions

R.B. conceived and designed the material. R.M., L.L., J-P.B. and M.A. performed the synthesis and characterization of the anionic monomers. S.M., L.L., T.N.T.P., D.G. and D.B. performed the synthesis and macromolecular characterization of the polyanionic block copolymers. S.M. and R.D. carried out the thermal analysis. A.A., D.D., R.D. and. R.B. performed the sample and battery preparation, the conductivity and mechanical measurements and electrochemical characterizations. R.B. analysed the data and wrote the paper. All authors discussed the results and commented on the manuscript.

Additional information

Supplementary information is available in the online version of the paper. Reprints and permissions information is available online at www.nature.com/reprints. Correspondence and requests for materials should be addressed to R.B.

Competing financial interests

The authors declare no competing financial interests.